ACS APPLIED MATERIALS & INTERFACES

Research Article

www.acsami.org

Laminated Adsorbents with Very Rapid CO_2 Uptake by Freeze-Casting of Zeolites

Arto Ojuva,*[,†,‡] Farid Akhtar,[†,‡] Antoni P. Tomsia,[§] and Lennart Bergström*[,†]

[†]Department of Materials and Environmental Chemistry and [‡]Berzelii Center EXSELENT on Porous Materials, Stockholm University, Stockholm 10691, Sweden

[§]Materials Sciences Division, Lawrence Berkeley National Laboratory, Berkeley, California 94720, United States

Supporting Information

ABSTRACT: Structured zeolite 13X monoliths with a laminated structure and hierarchical macro-/microporosity were prepared by freeze-casting aqueous suspensions of zeolite 13X powder, bentonite, and polyethylene glycol. Colloidally stable suspensions with a low viscosity at both room temperature and near freezing could be prepared at alkaline conditions where both the zeolite 13X powder and bentonite carry a negative surface charge. Slow directional freezing of the suspensions led to the formation of well-defined and thin lamellar pores and pore walls while fast freezing resulted in more cylindrical pores. The wall thickness, which varied between 8 and 35 μm, increased with increasing solids loading of the suspension. Thermal treatment at 1053 K of the freeze-cast bodies containing between 9 and 17 wt % bentonite resulted in mechanically stable zeolite 13X monoliths. The monoliths displayed a carbon dioxide uptake capacity of 4−5 mmol/g and an uptake kinetics characterized by a very fast initial uptake where more than 50% of the maximum uptake was reached within 15 s. Freeze-cast laminated zeolite monoliths could be used to improve the volumetric efficiency and reduce the cycle time, of importance in, for example, biogas upgrading and CO_2 separation from flue gas.

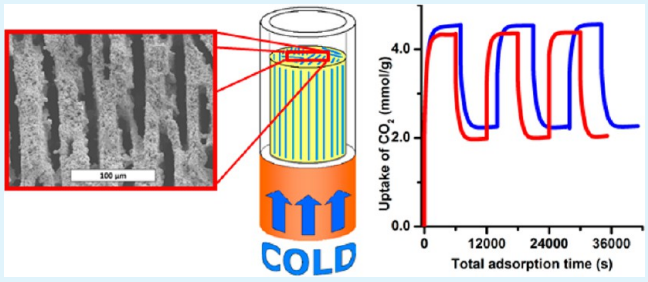

KEYWORDS: *freeze-casting, zeolite 13X, shaping, structured, laminate, adsorbent, hierarchical, carbon dioxide, CCS, gas separation, uptake kinetics*

INTRODUCTION

Microporous adsorbents, e.g., zeolites,[1,2] porous carbons,[3,4] and metal organic frameworks,[5,6] are widely used in industrially important separation processes, e.g., separation of oxygen/nitrogen from air,[7] and have also recently received considerable attention for carbon dioxide (CO_2) capture[8,9] and biogas upgrading.[10] One of the most studied materials for CO_2 capture is zeolite 13X, which possesses an interesting combination of low cost, high CO_2-uptake capacity, high CO_2 over N_2 selectivity, and good thermal and mechanical stability.[11−13]

Cost- and energy-effective gas separation requires that the microporous powder is structured into a macroscopic shape with a sufficient mechanical, chemical and attrition resistance that promotes high gas flows and rapid mass transfer.[14,15] Zeolites are often structured into beads, granules and pellets using processing techniques like extrusion, spray-drying, or granulation where the zeolite is normally mixed with an inorganic and organic binder, shaped into the desired geometry and thermally treated to remove the organic binder and impart mechanical strength by the inorganic binder. However, diluting the active component (the zeolite grains) with an inert binder invariably reduces the uptake capacity per unit weight. In addition, high pressure drop associated with gas flow through packed beds of beads or pellets and mass transfer limitations related to slow gas diffusion in and out of the granules or pellets are limiting the performance, in particular for large-scale applications. Structured adsorbents of various types, e.g., monolith, laminate, and foam, have recently attained considerable interest as more efficient alternatives and Rezaei and Webley[15,16] recently identified the parameters which have an important influence on the performance in large-scale gas separation processes, e.g., CO_2 capture and biogas upgrading. The parameters that relate to the structure of the adsorbent include: (i) the amount of adsorbent contained in a given volume (the adsorbent loading or the volume efficiency), (ii) the external surface area per unit volume, and (iii) the total void volume. Their mathematical analysis showed that laminate systems are very promising if the pore width (the spacing) and sheet widths (the wall thickness) is sufficiently small (below 200 μm). For example, using the Ergun[17] and Hagen−Poiseuille[18] equations, the pressure drop for a laminated structure with a spacing and wall thickness of 0.2 mm is an order of magnitude smaller than for a bed of 0.7 mm beads. If the spacing and wall thickness can be further reduced to, for

Received: January 10, 2013
Accepted: March 13, 2013
Published: March 13, 2013

example, 0.02 mm, a laminar structure will show a smaller pressure drop than a packed bed when the flow rate exceeds 3 $\times 10^{-9}$ m^3/s.

Structured adsorbents can be produced by a range of methods, e.g., by coating a support structure, such as extruded honeycombs[18,19] or ceramic foams,[20,21] by various assembly,[22] postsynthesis,[23] or leaching methods,[24] or by sacrificial templating[25−27] using polymers,[28] surfactants,[29] carbon,[30] ice,[31] and sponges.[32] Coated honeycomb monoliths allow large gas flows but the relative weight of the support material is high and the pore channels are large, which limits the weight and volume efficiency. Self-supported sacrificially templated structured adsorbents, where the microporous powder is the dominating component, have the potential to maximize the volume efficiency providing that the void volume is sufficiently small.

Ice-templating, commonly known as freeze-casting, offers a versatile approach for shaping porous inorganic monoliths with a high open porosity and a lamellar or laminate-like structure.[31] Controlled freezing of a suspension results in segregation of ice crystals and dense particle-rich domains that can be separated by subliming the ice and leaving a green body with continuous residual ice-templated pores. Deville and co-workers, along with others, have demonstrated how macroporous alumina materials with highly anisotropic microstructures can be produced by controlling the freezing front velocity and the composition of the dispersion.[33−35] Freeze-casting has been used to prepare porous scaffolds and bioceramics[36,37] but the reports on the use of freeze-casting to shape structured adsorbents are sparse. Mori et al.[38] have recently reported a two-step process to produce a porous silica monolith with a microporous surface layer by freeze-casting a silica precursor into an open columnar structure, followed by hydrothermal conversion of the surface layer into a microporous SiO_2-adsorbent, silicalite-1.

This work aims to demonstrate how freeze-casting dispersions of microporous zeolite powders can be used as a versatile shaping method to produce structured adsorbents with a laminated structure with pore widths and wall thicknesses less than 20 μm. The influence of particle concentration and cooling rate on the structural features and the mechanical strength has been investigated by scanning electron microscopy (SEM), Hg-porosimetry and compressive strength measurements, respectively. The carbon dioxide uptake kinetics was determined and the relative contribution of the macrostructure and the dimensions of the zeolite crystal were analyzed and discussed.

MATERIALS AND METHODS

Zeolite 13X with a particle size of 3−5 μm was obtained from Luoyang Jianlong Chemical Industrial Co., LTD, China. Bentonite clay (Sigma-Aldrich Chemie GmbH, Buchs, Germany) was used as the inorganic binder and polyethylene glycol (PEG) (MW = 8000, Sigma-Aldrich Chemie GmbH, Buchs, Germany) was used as the sacrificial organic binder prior to thermal treatment.

The freeze-casting unit consisted of a nitrogen vessel with a protruding copper rod for heat transfer, similar to the unit used by Deville and co-workers.[39] The copper rod was fitted with a thermocouple and a heater, which enabled the temperature and the cooling rate to be controlled. The suspensions for freeze-casting were prepared from zeolite 13X powder, bentonite and polyethylene glycol mixed in deionized water. The suspensions were alkaline (pH 9−10) without any addition of base.

The suspensions were characterized with respect to the amount of added inorganic mass divided by the total weight, excluding the temporary organic binder (PEG), expressed as wt% dwb (dry weight basis), and also with respect to the relative amount of inorganic binder bentonite in wt%, expressed as the mass of bentonite divided by the total mass of the inorganic powders (zeolite 13X+bentonite). We have freeze-cast structured adsorbents from 6 different suspensions: suspensions of 27.8 wt % dwb, 30.2 wt % dwb and 32.4 wt % dwb containing 9.1 wt % bentonite and suspensions of 27.9 wt %, 30.3 wt %, and 32.4 wt % dwb containing 16.7 wt % bentonite, as shown in Table 1. The mass of the added organic binder PEG was always 10 wt % of the mass of the added zeolite 13X.

Table 1. Relative Amounts of the Components Zeolite 13X, Bentonite, Polyethylene Glycol (PEG), and Water That the Suspensions Contain Prior to Freeze-Casting

	27.8 wt % dwb	30.2 wt % dwb	32.4 wt % dwb	27.9 wt % dwb	30.3 wt % dwb	32.4 wt % dwb
zeolite 13X (g)	36.4	40.9	45.5	33.3	37.5	41.7
bentonite (g)	3.64[a]	4.09[a]	4.55[a]	6.66[b]	7.50[b]	8.34[b]
PEG (g)	3.64	4.09	4.55	3.33	3.75	4.17
H_2O (mL)	100	100	100	100	100	100

[a]Corresponds to an addition of 9.1 wt % bentonite. [b]Corresponds to an addition of 16.7 wt % bentonite.

The monoliths were prepared by mixing zeolite 13X and bentonite powders with PEG and water in a polypropylene flask. The mixture was ball milled for 6 h with 5 mm alumina balls. It was then poured into a flask and subjected to a low vacuum under stirring to remove air. Small aliquots of the homogenized and de-aired suspensions, typically 6−8 mL at a time, were then put in a cylindrical Teflon mold (inner diameter 20.0 mm) with a copper bottom-piece that was placed onto the protruding copper rod of the freeze-casting unit. The temperature was initially reduced to 276 K and held at that temperature for 3 min. The suspensions were then allowed to freeze at a controlled cooling rate that was varied between 0.5 and 5 K/min. When the temperature reached 233 to 193 K, depending on the cooling rate, the frozen bodies were removed from the Teflon mold and put in a freeze-drier (Hetosic, Heto lab equipment, Denmark) for 2 days.

The freeze-dried powder bodies were thermally treated in an oven where the temperature was increased by 2 K/min up to 823 K, where the temperature was held for two hours to burn out the organic binder, and then further increased at a heating rate of 10 K/min up to 1053 K. The powder body was then allowed to be cooled down at a cooling rate of 10 K/min down to room temperature.

The steady-shear viscosity of the suspensions was measured at 278, 288, and 298 K with a Paar Physica MCR301 (Anton Paar GmbH, Graz, Austria) with a concentric cylinder geometry. All suspensions were presheared in the rheometer at 50 s^{-1} for 3 min and then allowed to equilibrate under no shear for 30 s prior to the commencement of the measurements. The suspensions were subjected to two measurement cycles, each consisting of 41 measurements at specific shear rates. The first cycle went from 0.1 to 1000 s^{-1}, with a 30 s measurement time for the first point and 2 s for the final, for a total of 430 s, and the second cycle was performed in the opposite direction starting from 1000 s^{-1} and ending in 0.1 s^{-1}.

Scanning electron microscope images were obtained with a JEOL JSM-7001F microscope (Jeol Ltd., Tokyo, Japan). Representative pieces were prepared from the middle of the monolith and cut into a suitable size (a few mm) with a scalpel. The piece of the hierarchically porous monolith was mounted on a metal plate with Leit-C conductive carbon cement (Plano GmbH, Wetzlar, Germany) and coated with a thin layer of gold prior to insertion into the microscope.

The compressive strengths of zeolite 13X monoliths with 9.1 wt % bentonite were measured in the freezing (axial) direction in a servo-hydraulic testing machine (MTS810, MTS Systems, Eden Prairie, MN). The monolith was compressed at a constant speed of 0.20 mm/min and the force was measured until the monolith broke.

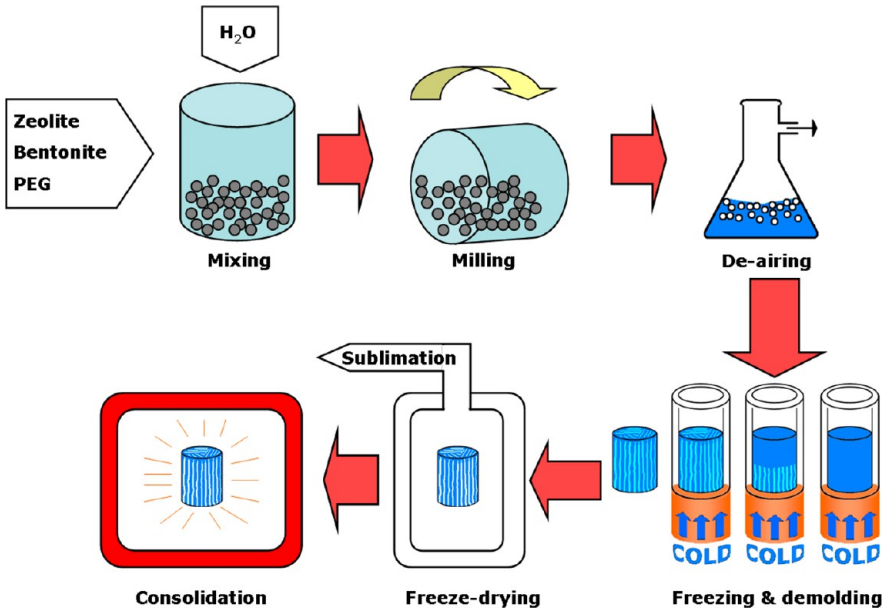

Figure 1. Schematics of the freeze-casting process. The zeolite 13X and bentonite powders were mixed with poly ethylene glycol (PEG) in water, ball milled overnight, and de-aired. The aqueous suspension was then poured into a cylindrical Teflon mold placed onto a heat-conducting metal plate. The freeze-cast cylinder was removed from the mold and transferred to a freeze-dryer where the ice was removed by sublimation.

Mercury intrusion porosimetry was performed on a small part of the monolith (about 0.5 g) with an AutoPore III 9410 (Micromeritics, Atlanta, GA). The pore size distribution was obtained from the Washburn equation[40] that describes the pressure p required to force mercury into a capillary pore of radius r

$$p = \frac{-2\gamma\cos\theta}{r} \quad (1)$$

where γ is the surface tension of mercury, taken to be 0.485 N/m, and θ is the contact angle of mercury, given as 130°. The maximum pressure attainable with the instrument is 414 MPa, which corresponds to pores of 3.0 nm in diameter (d), but tests revealed that there is no intrusion above 100 MPa (d = 13 nm), so the maximum pressure for most of the measurements were kept at 240 MPa (d = 5 nm).

Carbon dioxide adsorption and desorption isotherms were measured at 293 K on an ASAP 2020 (Micromeritics Instrument Corporation, Norcross, GA). The temperature was controlled by a CF31 cryo-compact circulator (Julabo Labortechnik GmbH, Seelbach, Germany) during the measurement. Two pieces from each monolith, approximately 4 × 4 × 8 mm, were cut from the middle of the monolith, degassed in vacuum at 573 K for 5 h and backfilled with nitrogen before measurement. The equilibrium adsorption−desorption cycles were measured in the CO_2 pressure regime of 0.011 to 101.3 kPa.

Two reference pellets were produced from a 32.4 wt % dwb suspension containing 9.1 wt % or 16.7 wt % bentonite. The suspensions were mixed and milled and then allowed to dry at 353 K, ground into a fine powder and dry pressed in a cylindrical die of diameter 21 mm, at an applied uniaxial pressure of 20 MPa. The pressed cylindrical composites were thermally treated using the same heating program as for the freeze-cast monoliths.

The time-dependent CO_2 adsorption and desorption were measured gravimetrically with a magnetic suspension balance (Rubotherm Präzisionsmesstechnik GmbH, Bochum, Germany) in a pressure chamber. The structured zeolite 13X monoliths (with a weight of 3−4 g) were placed in a closed chamber and evacuated at 573 K for 5 h in vacuum prior to measurement. Three measurement cycles were made at 303 K, each consisting of an uptake step and a desorption step. In the uptake step, CO_2 was rapidly introduced and the pressure was maintained at 140 kPa while the mass of the monolith was continuously recorded using a microbalance until the material had reached full saturation. In the desorption step, the pressure was dropped to 5 kPa and the mass was monitored until steady-state was reached.[41]

RESULTS AND DISCUSSION

We have prepared laminate-structured zeolite 13X-monoliths with an open macroporosity and a very rapid initial uptake of CO_2 by freeze-casting. The composite bodies were prepared from suspensions containing zeolite 13X powder, bentonite, and polyethylene glycol as shown in Figure 1.

Measurements of the steady-shear rheological behavior of the deagglomerated and ball-milled aqueous suspensions (Figure 2a) show that an increase of the bentonite content from 9.1 wt % to 16.7 wt % (while keeping the total solids loading constant at 32.4 wt % dwb) increases the viscosity about 3 times and also changes the rheological behavior from Newtonian to weakly

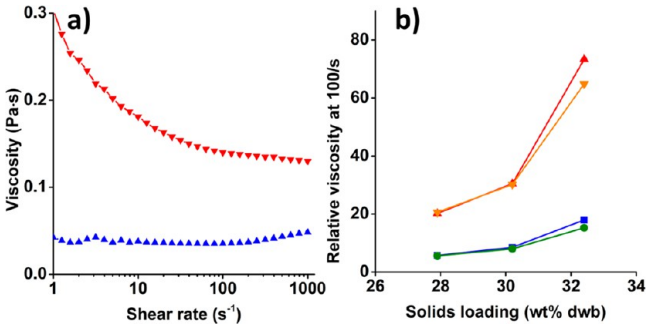

Figure 2. Steady-shear viscosity of aqueous suspensions. (a) Steady-shear viscosity of suspensions of zeolite 13X, bentonite, and the organic binder PEG at 298 K at a solids loading of 32.4 wt % dwb and a bentonite content of 9.1 wt % (blue up-facing triangle), and 16.7 wt % (red down-facing triangle). (b)Relative viscosity (η/η_s) at a shear rate of 100/s versus inorganic solids loading (in wt% dwb) for suspensions containing 9.1 wt % bentonite at temperatures of 298 K (green circle) and 278 K (blue square), and for suspensions containing 16.7 wt % bentonite at 298 K (orange down-facing triangle) and 278 K (red up-facing triangle).

dx.doi.org/10.1021/am400122r | ACS Appl. Mater. Interfaces 2013, 5, 2669−2676

shear thinning. Bentonite is a typical clay binder for zeolite monoliths[42] and its effect on the rheological properties can be related to its platelike morphology: previous work has shown that highly anisotropic particles, e.g., platelike clays[43] and rodlike whiskers,[44] increase the viscosity and induce a non-Newtonian behavior at significantly lower concentrations compared to more equiaxed particles. However, the effect is relatively weak and the suspensions prepared at both high and low additions of bentonite are nonaggregated. The colloidal stability can be related to the negative surface charge of both bentonite and zeolite 13X at the investigated alkaline pH; bentonite has an isoelectric point pH_{iep} 8.0[45] and zeolite 13X has an isoelectric point pH_{iep} 4.7.[13]

The insignificant difference in the relative viscosity $\eta_r = \eta/\eta_s$, where η_s is the viscosity of the solvent (H_2O+PEG), at 278 and 298 K in Figure 2b, indicates that the colloidal stability is maintained also when the temperature is reduced to 278 K. This is important as successful freeze-casting of well-defined structured materials requires that agglomeration is avoided and that the particles can be transported by the freezing front.[35,46]

The freeze-cast zeolite 13X powder bodies have been thermally treated at a temperature of 1053 K. Thermal treatment at this carefully selected temperature promotes an increase of the strength through the formation of thermally activated bonds while avoiding excessive melting or sintering that could substantially decrease the surface area and thus reduce the uptake capacity of the zeolite.[47] Figure 3 shows that

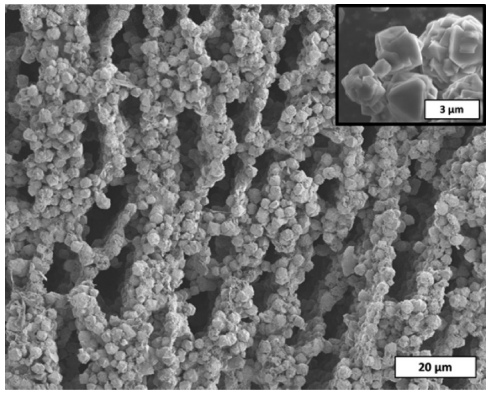

Figure 3. Scanning electron micrographs of a freeze-cast zeolite 13X monolith. The monolith was prepared from a zeolite/bentonite suspension with an initial concentration of 30.2 wt % dwb and a cooling rate of 5 K/min. The cross-section is perpendicular to the freezing direction. Inset shows the as-received zeolite 13X powder.

the original morphology of individual zeolite 13X particles is preserved after the thermal treatment, suggesting that the temperature is too low to induce any significant melting or sintering. Figure 4 shows that the freeze-cast and thermally treated zeolite 13X monoliths display an uptake of carbon dioxide that is about 75−80% of the uptake of the pure powder. The surface area, measured by nitrogen adsorption at 77 K (see the Supporting Information, Figure S2), is reduced from 780 m^2/g for the untreated 13X powder to 670 m^2/g for the heat treated monoliths. Indeed, if we compensate for the addition of 9.1 wt % of the inert bentonite binder, the surface area of the 13X zeolite is only reduced by 6% by the heat treatment to 1053 K.

Previous work[46,48] has shown that the strong difference in growth rates for the different faces of ice yields freeze-cast

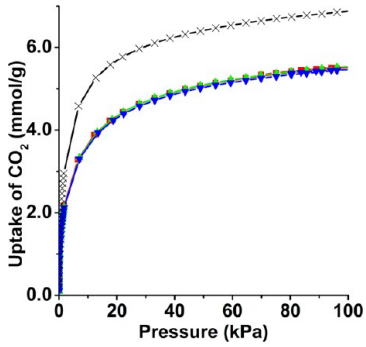

Figure 4. Adsorption isotherms of carbon dioxide on zeolite 13X monoliths and powder. Carbon dioxide uptake against pressure of zeolite 13X powder (black x) and zeolite 13X monoliths prepared from a suspension with 9.1 wt % bentonite at different cooling rates: 0.5 K/min (red square), 1 K/min (green up-facing triangle), and 5 K/min (blue down-facing triangle). All isotherms were measured at 298 K.

materials with a strongly anisotropic microstructure. Figure 5 gives an overview of how the microstructures of the freeze-cast materials depend on the solids loading and the cooling rate. The growth of large anisotropic ice crystals along the temperature gradient results at slow cooling rates (0.5 and 1 K/min) in elongated, lamellar ice crystals[34] that after ice removal yields anisotropic pores with a width of 10−20 μm, separated by granular, platelike walls with a thickness of 8−35 μm consisting of dense-packed zeolite 13X particles and bentonite.

Increasing the cooling rate of 0.5 or 1 K/min to 5 K/min results in a transition from lamellar to columnar pore structures for the two most concentrated suspensions (30.2 and 32.4 wt % dwb). The transition is probably related to an insufficient mobility of the dispersed particles which leads to early entrapment of the suspended particles in the advancing freezing front.[33] The ice growth is confined to columnar structures, which yields cylindrical pores with diameters varying between 5 and 10 μm. The granular walls are not well-defined but the characteristic wall thickness is relatively small as the separation distance between two cylindrical pores does not exceed 10 μm.

The main effect of the solids content of the suspension on the microstructure is an increase of the thickness of granular walls with increasing concentration. The addition of bentonite at the relative concentrations investigated in this study did not have any significant effect on the microstructure (not shown).

The SEM observations in Figure 5 show that the pore dimensions of the freeze-cast monoliths are largest for the materials freeze-cast at the lowest cooling rate. This is corroborated by the mercury intrusion data in Figure 6, which shows that monoliths frozen at 5 K/min show the smallest pores with a mean diameter of 7 μm, whereas monoliths frozen at 0.5 K/min show the largest pores with a mean diameter of 15 μm. All of the freeze-cast zeolite 13X monoliths display a bimodal pore size distribution where the smaller pores with an average diameter around 1 μm can be related to the interparticle pores between the zeolite 13X particles, which have a diameter of 3−5 μm.

The compressive strength of freeze-cast monoliths containing 9.1 wt % bentonite (Table 2) varies between 54 and 690 kPa depending on the initial solids loading and the cooling rate. The compressive strength, σ_{cr}, of an isotropic cellular porous

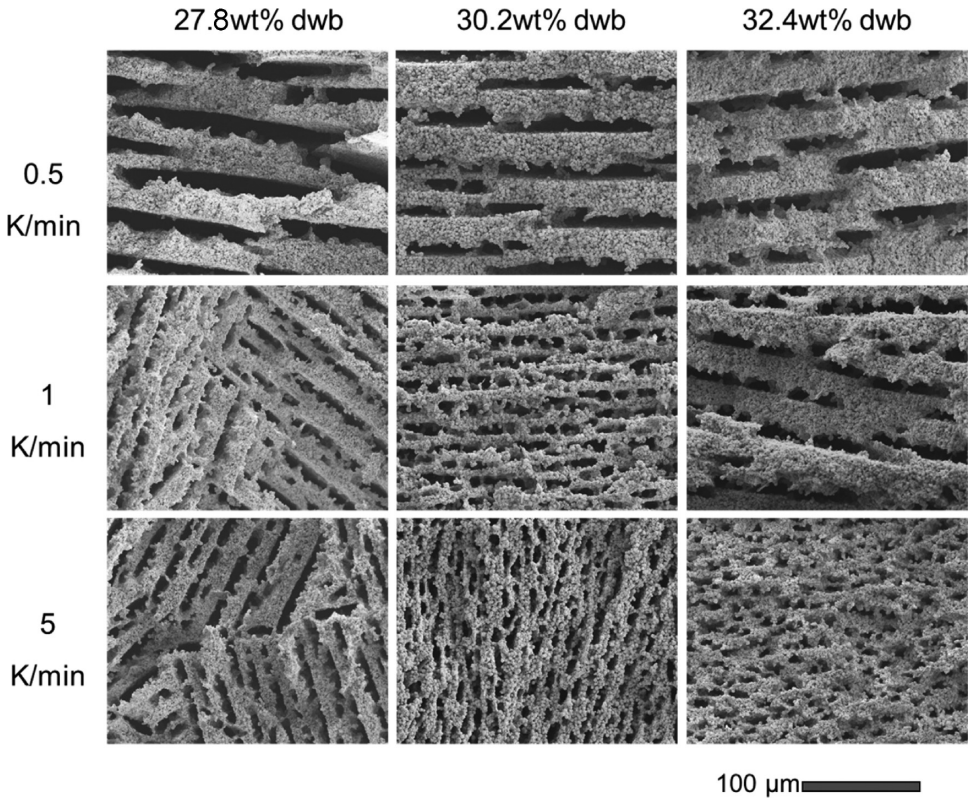

Figure 5. Microstructures of freeze-cast zeolite 13X monoliths. SEM images of freeze-cast monoliths prepared from suspensions of different solids loading (wt % dwb of inorganic components) and cooling rates. The materials contain 9.1 wt % bentonite.

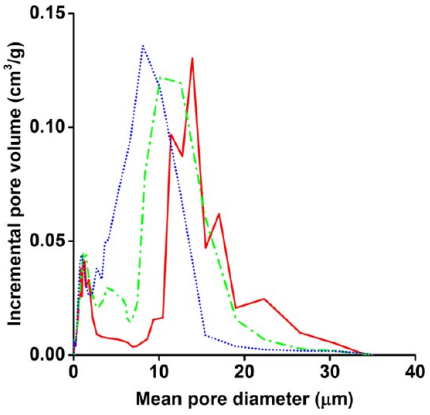

Figure 6. Mercury intrusion in freeze-cast monoliths. The incremental pore volume is plotted against the mean diameter of an equivalent cylindrical pore for freeze-cast monoliths prepared from a suspension with solids loading of 32.4 wt % dwb and a bentonite content of 9.1 wt %. The different colors represent monoliths prepared at a cooling rate of: 0.5 K/min (red solid line), 1 K/min (green dash-dot line), 5 K/min (blue dotted line).

Table 2. Compressive Strengths of Freeze-Cast Zeolite 13X Monoliths Containing 9.1 wt % Bentonite

total inorganic wt % dwb	compressive strength (kPa)		
27.8	54[a]	100[b]	130[c]
30.2	80[a]	280[b]	390[c]
32.4	77[a]	100[b]	690[c]

[a]Frozen at 0.5 K/min. [b]Frozen at 1 K/min. [c]Frozen at 5 K/min.

structure is expected to be proportional to the area fraction of solids, i.e., $(\rho/\rho_s)^{3/2}$, where ρ is the density of the porous structure and ρ_s is the density of the solid walls.[37,49] Although Table 2 suggests that the compressive strength is higher for the monoliths prepared from suspensions with a higher solids loading, the large scatter in the data prohibits a more detailed analysis. We speculate that the pronounced anisotropy of the freeze-cast structures and problems related to sample preparation and acquiring accurate measurements from these relatively fragile materials is related to the scatter in the data.

The mechanical strength of the monoliths should be sufficiently high to withstand handling, transport, and the stresses induced by the pressure gradients induced, for example, in a vacuum swing adsorption (VSA) operation. In this context, strengths above a few 100 kPa, obtained, for example, by monoliths free-cast at cooling rates of 5 K/min (Table 2), were sufficient for the monoliths to withstand repeated cyclic testing where the pressures varied between 5 and 140 kPa (see below).

We have investigated the uptake kinetics by repeatedly subjecting the freeze-cast zeolite 13X monoliths to a typical VSA cycle where CO_2 is allowed to adsorb at 140 kPa and the material is regenerated at 5 kPa at 303 K. Figure 7 shows that uptake during the first adsorption cycle is significantly higher than the uptake during the consecutive cycles. This effect has been observed previously and can be related to chemisorption and/or strong physisorption of CO_2.[50] Regeneration at a pressure of 5 kPa is thus unable to remove all the adsorbed CO_2 and the maximum adsorption capacity becomes 2.7 mmol/g (for monoliths containing 9.1 wt % bentonite) and 2.3 mmol/g (for monoliths containing 16.7 wt % bentonite) beyond the first cycle. After the first cycle, the CO_2 adsorption

dx.doi.org/10.1021/am400122r | ACS Appl. Mater. Interfaces 2013, 5, 2669−2676

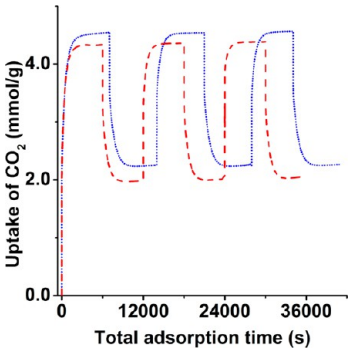

Figure 7. Time-resolved vacuum swing adsorption measurements on freeze-cast zeolite 13X monoliths: The adsorption and desorption of CO_2 at 303 K is shown for three consecutive cycles for zeolite 13X monoliths freeze-cast from suspensions at a cooling rate of 0.5 K/min and a solids loading of 30.2 wt % dwb with a bentonite addition of 9.1 wt % (blue dotted line) and 30.3 wt % dwb with a bentonite addition of 16.7 wt % (red dashed line). The adsorption was performed at a pressure of 140 kPa and desorption at a pressure of 5 kPa.

capacity of the monoliths remains unchanged in the following adsorption and desorption cycles.

The CO_2 uptakes in Figure 8 represent the time-dependent adsorption data from the second cycle where the contribution

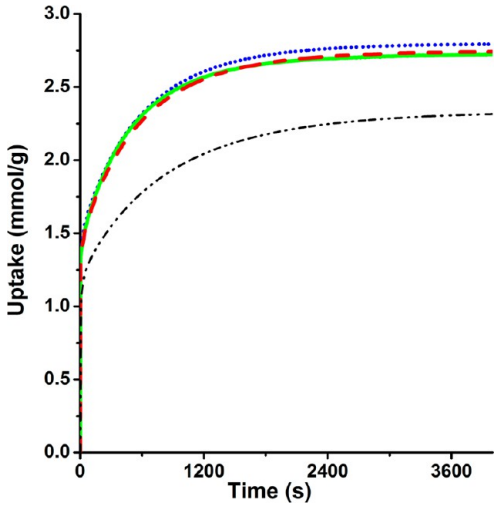

Figure 8. Time-dependent CO_2 uptake of freeze-cast zeolite 13X monoliths. The time-dependent uptake of CO_2 at a pressure of 140 kPa is shown for zeolite 13X monoliths containing 9.1 wt % bentonite. The monoliths were prepared from suspensions at a cooling rate of 1 K/min with solids loadings of: 27.8 wt % (blue dotted line), 30.2 wt % (green solid line), and 32.4 wt % (red dashed line) dwb. The time-dependent uptakes for pressed and thermally treated cylindrical pellets with corresponding amount of bentonite are shown for comparison (black dash-dot line).

from chemisorption is negligible. All the freeze-cast monoliths are characterized by a very fast initial uptake followed by a slower time-dependent uptake up to saturation which is about 2.7 mmol/g at the VSA parameters used in this study. The freeze-cast zeolite monoliths with 9.1 wt % bentonite adsorb 1.4 mmol/g CO_2, i.e., 50% of their full capacity, in less than 10 s. In comparison, the pressed monolith shows a slower rate of CO_2 adsorption and requires 160 s to adsorb CO_2 50% of its full capacity. Recent calculations by Rezaei and Webley[16] suggest that laminated structures with pore and wall widths lower than 200 μm could be very favorable for rapid gas uptake and release. The fast initial uptake can be related to the small resistance to gas flow and the large available external surface area of the thin walls, which allows the gas to rapidly come in contact with the zeolite particles.

The freeze-cast monoliths that contain a higher amount (16.7 wt %) of bentonite display a lower uptake that is also more scattered compared to the freeze-cast monoliths, see the Supporting Information, Figure S3. Hence, our results strongly indicate that the amount of the inorganic binder should be kept as low as the demands for mechanical strength permit.

The long-time uptake for all the freeze-cast materials can be described by an exponential decay function that is related to an expression describing diffusion in porous spheres. For a spherical particle of radius r the uptake m can be described by the isothermal expression[51,52]

$$\frac{m_t}{m_\infty} = 1 - \frac{6}{\pi^2}\sum_{n=1}^{\infty}\frac{1}{n^2}\exp\left(-\frac{n^2\pi^2 Dt}{r^2}\right) \quad (2)$$

where D is the particle diffusivity. For uptakes greater than 70% it is possible to use the long-time approximation

$$1 - \frac{m_t}{m_\infty} \approx \frac{6}{\pi^2}\exp\left(-\frac{\pi^2 Dt}{r^2}\right) \quad (3)$$

that we have used to determine the diffusivity from a plot of $\ln(1 - m/m_\infty)$ versus t. The analysis from the third adsorption cycle of all freeze-cast monoliths yielded a diffusivity of 7×10^{-16} m^2/s at 303 K, which is several orders of magnitude lower than reported values for the intracrystalline self-diffusion in zeolite 13X determined by ^{129}Xe and ^{13}C PFG NMR at isothermal conditions (Kärger et al.,[53] $D = 9 \times 10^{-8}$ m^2/s). However, it is in good agreement with the diffusivity values obtained previously by uptake measurements similar to a study for pellets with more pronounced intercrystalline diffusion; Silva et al.[12] reported $D = 10.9 \times 10^{-16}$ m^2/s for binderless zeolite 13X beads at 313 K. This large discrepancy suggests that the uptake is greatly affected by other factors, such as heat dissipation from the particles.

CONCLUSIONS

Freeze-casting of aqueous suspensions of zeolite 13X, bentonite, and polyethylene glycol was used to produce volume-efficient structured adsorbents that displayed a very fast uptake of CO_2. Preparation at an alkaline pH resulted in colloidally stable suspensions that displayed a Newtonian or only weakly shear thinning behavior and a relatively low viscosity also at low temperatures. We showed how the cooling rate and the solids loading of the suspension controls the microstructure of the freeze-cast monoliths and identified the parameters for the production of laminated monoliths, i.e., cooling rates below 5 K/min. The wall thickness could be varied between 8 and 35 μm and the pore width between 5 and 20 μm, depending on the solids loading. The effect of the bentonite which acts as an inorganic binder showed that increasing the bentonite content reduced the maximum CO_2 uptake capacity of the monoliths as the active component, zeolite 13X, was diluted.

Laminated monoliths with thin pore widths and walls were recently identified as particularly interesting structures for improving the volumetric efficiency and reducing the cycle time. The freeze-cast zeolite monoliths displayed a high carbon

dioxide uptake capacity and a very fast initial uptake where more than 50% of the maximum uptake was obtained within 10−20 s. This fast initial uptake was related to the small resistance to gas flow and the large external surface area of the thin, granular walls that allowed the gas to rapidly come in contact with the zeolite particles.

The freeze-cast zeolite monoliths are to our knowledge the first examples of laminated adsorbents with dimensions suitable for substantial improvement of the volumetric efficiency and reduction of the cycle time, which is of great importance in large-scale gas separation processes, e.g., biogas upgrading and CO_2 capture. This first study could pave the way for future investigations where the strength is improved further using molecular inorganic binders and the uptake rate is increased by using zeolite particles with a smaller particle size.

■ ASSOCIATED CONTENT

Supporting Information

Powder X-ray diffraction data for the as-received zeolite 13X powder and a monolith prepared by freezing a 30.2 wt % dwb solid containing 16.7 wt % bentonite, at 5 K/min. Nitrogen adsorption isotherms at 77 K. The time-dependent uptake of CO_2 at a pressure of 140 kPa for zeolite 13X monoliths containing 9.1 wt % bentonite. This material is available free of charge via the Internet at http://pubs.acs.org.

■ AUTHOR INFORMATION

Corresponding Author

*E-mail: lennart.bergstrom@mmk.su.se.

Funding

Notes

The authors declare no competing financial interest.

■ ACKNOWLEDGMENTS

This work has been financed by Berzelii Center EXSELENT on Porous Materials. Part of this work was supported by the Director, Office of Science, Office of Basic Energy Sciences, Division of Materials Sciences and Engineering, of the U.S. Department of Energy under Contract DE-AC02−05CH11231. The authors thank Dr. Manuel Houmard for valuable advice and help with the freeze-cast apparatus and compressive strength tests and Mrs. Grace Lau for technical assistance at the Materials Sciences Division at the Lawrence Berkeley National Laboratory. The cyclic sorption tests for uptake kinetics were performed by Dr. Andreas Möller at Institut für Nichtklassische Chemie, Leipzig, Germany.

■ REFERENCES

(1) Derouane, E. G. *J. Mol. Catal. A: Chem.* **1998**, *134*, 29−45.
(2) Samanta, A.; Zhao, A.; Shimizu, G. K. H.; Sarkar, P.; Gupta, R. *Ind. Eng. Chem. Res.* **2011**, *51*, 1438−1463.
(3) Ryoo, R.; Joo, S. H.; Kruk, M.; Jaroniec, M. *Adv. Mater.* **2001**, *13*, 677−681.
(4) Chue, K. T.; Kim, J. N.; Yoo, Y. J.; Cho, S. H. *Ind. Eng. Chem. Res.* **1995**, 591−598.
(5) Reineke, T. M.; Eddaoudi, M.; O'Keeffe, M.; Yaghi, O. M. *Angew. Chem., Int. Ed.* **1999**, *38*, 2590−2594.
(6) Li, J.-R.; Kuppler, R. J.; Zhou, H.-C. *Chem. Soc. Rev.* **2009**, *38*, 1477−1504.
(7) Li, Y. Y.; Perera, S. P.; Crittenden, B. D. *Chem. Eng. Res. Des.* **1998**, *76*, 921−930.
(8) D'Alessandro, D. M.; Smit, B.; Long, J. R. *Angew. Chem., Int. Ed.* **2010**, *49*, 6058−6082.
(9) Hedin, N.; Andersson, L.; Bergström, L.; Yan, J. *Appl. Energy* **2013**, *104*, 418−433.
(10) Cosoli, P.; Ferrone, M.; Pricl, S.; Fermeglia, M. *Chem. Eng. J.* **2008**, *145*, 86−92.
(11) Ko, D.; Siriwardane, R.; Biegler, L. T. *Ind. Eng. Chem. Res.* **2003**, 339−348.
(12) Silva, J. A. C.; Schumann, K.; Rodrigues, A. E. *Microporous Mesoporous Mater.* **2012**, *158*, 219−228.
(13) Akhtar, F.; Bergström, L. *J. Am. Ceram. Soc.* **2011**, *94*, 92−98.
(14) Rezaei, F.; Mosca, A.; Webley, P.; Hedlund, J.; Xiao, P. *Ind. Eng. Chem. Res.* **2010**, *49*, 4832−4841.
(15) Rezaei, F.; Webley, P. *Sep. Purif. Technol.* **2010**, *70*, 243−256.
(16) Rezaei, F.; Webley, P. *Chem. Eng. Sci.* **2009**, *64*, 5182−5191.
(17) Ergun, S. *Chem. Eng. Prog.* **1952**, *48*, 89−94.
(18) Cybulski, A.; Moulijn, J. A. *Catal. Rev.: Sci. Eng.* **1994**, *36*, 179−270.
(19) Nijhuis, T. A.; Beers, A. E. W.; Vergunst, T.; Hoek, I.; Kapteijn, F.; Moulijn, J. A. *Catal. Rev.: Sci. Eng.* **2001**, *43*, 345−380.
(20) Andersson, L.; Akhtar, F.; Ojuva, A.; Bergström, L. *J. Ceram. Sci. Tech.* **2012**, *3*, 9−16.
(21) Buciuman, F.-C.; Kraushaar-Czarnetzki, B. *Catal. Today* **2001**, *69*, 337−342.
(22) Yin, M.; Li, Z.; Liu, Z.; Yang, X.; Ren, J. *ACS Appl. Mater. Interfaces* **2012**, *4*, 431−437.
(23) Pavel, C. C.; Schmidt, W. *Chem. Commun.* **2006**, *5*, 882−884.
(24) Verboekend, D.; Pérez-Ramírez, J. *Chem.—Eur. J.* **2011**, *17*, 1137−1147.
(25) Stein, A.; Melde, B.; Schroden, R. *Adv. Mater.* **2000**, *12*, 1403−1419.
(26) Ohji, T.; Fukushima, M. *Int. Mater. Rev.* **2012**, *57*, 115−131.
(27) Akhtar, F.; Andersson, L.; Keshavarzi, N.; Bergström, L. *Appl. Energy* **2012**, *97*, 289−296.
(28) Antonietti, M.; Berton, B.; Göltner, C.; Hentze, H.-P. *Adv. Mater.* **1999**, *20*, 154−159.
(29) Bagshaw, S. A.; Prouzet, E.; Pinnavaia, T. J. *Science* **1995**, *269*, 1242−1244.
(30) Janssen, A. H.; Schmidt, I.; Jacobsen, C. J. H.; Koster, A. J.; De Jong, K. P. *Microporous Mesoporous Mater.* **2003**, *65*, 59−75.
(31) Deville, S. *Adv. Eng. Mater.* **2008**, *10*, 155−169.
(32) Colombo, P.; Vakifahmetoglu, C.; Costacurta, S. *J. Mater. Sci.* **2010**, *45*, 5425−5455.
(33) Deville, S.; Saiz, E.; Tomsia, A. P. *Acta Mater.* **2007**, *55*, 1965−1974.
(34) Bareggi, A.; Maire, E.; Lasalle, A.; Deville, S. *J. Am. Ceram. Soc.* **2011**, *94*, 3570−3578.
(35) Waschkies, T.; Oberacker, R.; Hoffmann, M. J. *Acta Mater.* **2011**, *59*, 5135−5145.
(36) Deville, S. *Materials* **2010**, *3*, 1913−1927.
(37) Wegst, U. G. K.; Schecter, M.; Donius, A. E.; Hunger, P. M. *Philos. Trans. R. Soc. London, Ser. A* **2010**, *368*, 2099−2121.
(38) Mori, H.; Aotani, K.; Sano, N.; Tamon, H. *J. Mater. Chem.* **2011**, *21*, 5677−5681.
(39) Munch, E.; Saiz, E.; Tomsia, A. P.; Deville, S. *J. Am. Ceram. Soc.* **2009**, *92*, 1534−1539.
(40) Washburn, E. W. *Proc. Natl. Acad. Sci. U.S.A.* **1921**, *7*, 115−116.
(41) Möller, A.; Pessoa Guimaraes, A.; Gläser, R.; Staudt, R. *Microporous Mesoporous Mater.* **2009**, *125*, 23−29.
(42) Dorado, F.; Romero, R.; Cañizares, P. *Ind. Eng. Chem. Res.* **2001**, *40*, 3428−3434.
(43) Sjöberg, M.; Bergström, L.; Larsson, A.; Sjöström, E. *Colloids Surf., A* **1999**, *159*, 197−208.
(44) Laarz, E.; Carlsson, M.; Vivien, B.; Johnsson, M.; Nygren, M.; Bergström, L. *J. Eur. Ceram. Soc.* **2001**, *21*, 1027−1035.
(45) Kim, D. S. *Environ. Eng. Res.* **2003**, *8*, 222−227.
(46) Lasalle, A.; Guizard, C.; Maire, E.; Adrien, J.; Deville, S. *Acta Mater.* **2012**, *60*, 4594−4603.
(47) Greaves, G. N.; Meneau, F.; Kargl, F.; Ward, D.; Holliman, P.; Albergamo, F. *J. Phys.: Condens. Matter* **2007**, *19*, 1−17.

(48) Deville, S.; Saiz, E.; Nalla, R. K.; Tomsia, A. P. *Science* **2006**, *311*, 515−518.
(49) Gibson, L. J. *J. Biomech.* **2005**, *38*, 377−399.
(50) Bertsch, L.; Habgood, H. W. *J. Phys. Chem.* **1963**, *67*, 1621−1628.
(51) Ruthven, D. M. In *Introducton to Zeolite Science and Practice*, 3rd revised ed.; Elsevier: Amsterdam, 2007; pp 743−744.
(52) Loughlin, K. F.; Derrah, R. I.; Ruthven, D. M. *Can. J. Chem. Eng.* **1971**, *49*, 66−70.
(53) Kärger, J.; Pfeifer, H.; Stallmach, F.; Feoktistova, N. N.; Zhdanov, S. P. *Zeolites* **1993**, *13*, 50−55.